Environmental Science and Pollution Research (2022) 29:17309–17318
https://doi.org/10.1007/s11356-021-17105-1

RESEARCH ARTICLE

Hydrogen peroxide–assisted photocatalytic dye degradation over reduced graphene oxide integrated $ZnCr_2O_4$ nanoparticles

Kartik Tantubay[1] · Piu Das[1] · Moni Baskey (Sen)[1]

Received: 10 August 2021 / Accepted: 14 October 2021 / Published online: 18 October 2021

Abstract

Zinc chromite nanoparticles (NPs) and zinc chromite–reduced graphene oxide ($ZnCr_2O_4$-rGO) nanocomposite have been synthesized by the combined effects of reflux condensation and calcination processes. The structural properties were characterized by X-ray diffraction (XRD), Fourier transform infrared (FTIR), UV–visible studies, etc. Structural morphology was investigated by field emission scanning electron microscopy (FE-SEM) and transmission electron microscopy (TEM) that indicate the formation of particles in the nanometer regime. The presence of the elements Zn, Cr, O and C has been confirmed by energy-dispersive X-ray spectroscopy (EDX) images which show the purity of the synthesized products. The photocatalytic activities of both as-prepared samples under visible light irradiation were investigated in presence of hydrogen peroxide (H_2O_2) and the results show that $ZnCr_2O_4$-rGO nanocomposite has a quite higher photo-activity response than virgin $ZnCr_2O_4$ NPs. The enhanced photo response indicates that, in $ZnCr_2O_4$, the photo-induced electrons favor to transfer to the rGO surface and the recombination of electron–hole pairs inhibited for which it results in the significantly increased photocatalytic activity for the $ZnCr_2O_4$-rGO photocatalyst and this phenomenon is also supported by the band gap value and photoluminescence results. Our outcomes demonstrate that $ZnCr_2O_4$-rGO nanocomposite is a more promising material to build up an efficient photocatalyst for waste water treatment.

Keywords $ZnCr_2O_4$-rGO · Nanocomposite · Catalytic activity · Methylene blue · Hydrogen peroxide

Introduction

The heterogeneous photocatalyst gives great promise for environmental contaminant elimination by transfer of photon energy into chemical energy (Nguyen et al. 2016; Kalisamy et al. 2020). The photocatalytic treatment for eradication of hazardous environmental pollutants, such as various organic dyes and chemical compounds, is one of the most efficient and economical concerns (Omidvar et al. 2017a, 2017b; Naghdi et al. 2018; Mohazzab et al. 2020; Jaleh et al. 2019; Nasrollahzadeh et al.2019; Ghosh et al. 2021a, 2021b). These pollutants egress from industries like textile, paper, food, cosmetic, pharmaceutical industries and contaminate water (Dong et al. 2015; Shang et al. 2014). So, the removal of these pollutants from water is very important for living beings (Nasrollahzadeh et al. 2021a, 2021b; Nasrollahzadeh et al. 2020; Nasrollahzadeh et al. 2021a, 2021b; Das et al. 2019; Ghosh et al. 2021a, 2021b). Graphene-based nanocomposites give auspicious results for the removing of the contaminants by catalytic (Anshuman et al. 2018; Tantubay et al. 2020), photocatalytic (Kocijan et al. 2021; Das et al. 2018; An and Yu 2011), adsorption (Chen et al. 2013; Dubey et al. 2015) and other processes due to its unique properties like large surface area (Singh et al. 2021), sp^2 hybridized carbon network (Gao et al. 2018), high electrical conductivity (Rahaman et al. 2020) and electron mobility (Gupta et al. 2020). There are several graphene-based photocatalysts such as, rGO-TiO_2 (Yu et al.2017), rGO-ZnO (Kumar et al. 2021), rGO-CuS/ZnS (Das et al. 2021), rGO-CuO (Gusain et al. 2016), rGO-NiO (Nafiey et al. 2017), rGO-Ag (Sen and Ghosh 2017), etc. for removing of organic dyes like methylene blue, rhodamine B, eosin-Y, congo red and crystal violet by using UV or visible light. But there are very few spinal

Responsible Editor: Sami Rtimi

✉ Moni Baskey (Sen)
moni.baskey@gmail.com

[1] Materials Research Laboratory, Department of Chemistry, The University of Burdwan, Golapbag, Burdwan, West Bengal 713104, India

nanocomposites reported for the removal of organic dyes from contaminant water.

There are much more spinel nanomaterials which showed their enhanced catalytic activities after being combined with graphene or reduced graphene oxide (Padhi et al. 2017; Amer et al. 2017; Gnanamoorthy et al. 2020; Krishnan et al. 2020). But zinc chromite ($ZnCr_2O_4$) is a less-studied material which behaves as a nanocatalyst in visible light irradiation and also there is no report about the synthesis of graphene or reduced graphene oxide functionalized $ZnCr_2O_4$ nanocomposite. Being a mixed oxide, it has a significant role in material science for its physical and chemical properties suitable for various applications. There are fewer literature surveys as described in Table 1 about the applications of $ZnCr_2O_4$ such as photocatalysis process for removal of various organic dyes (Dumitru et al. 2018; Sabet and Jahangiri 2018), catalytic application for thermal decomposition (Wang et al. 2020) and sensing property for explosive nitro compounds (Ghosh et al. 2018), humidity sensing (Pokhrel et al. 2003) but no one synthesizes the low-dimensional $ZnCr_2O_4$ nanomaterials which can respond in visible light to degrade organic dye. There are several methods for synthesis of $ZnCr_2O_4$ nanomaterials, such as thermal conversion (Dumitru et al. 2018), hydrothermal process (Sabet and Jahangiri 2018), sol–gel process (Choudhary et al. 2017), combustion process (Kumar and Chakra 2017) and reflux process (Tajizadegan et al. 2016). Out of these, reflux followed by calcination is a very simple and more cost-effective method to synthesize different nanomaterials.

Here, in this paper, about 4–7nm $ZnCr_2O_4$ NPs on reduced graphene oxide (rGO) surface have been synthesized by simple reflux method followed by calcination, and then after characterization by XRD, FTIR, UV–Vis, FESEM, TEM, PL studies the visible light–active photocatalytic activity for the degradation of methylene blue organic dye has been investigated.

Materials and methods

Materials

Zinc sulfate [$ZnSO_4$, $7H_2O$] (Merck), chromium nitrate [$Cr(NO_3)_3$, $9H_2O$] (Merck), polyvinyl pyrrolidone (PVP) (LOBA), ultrafine graphite powder (Sigma-Aldrich), conc. sulfuric acid (Merck), conc. hydrochloric acid (Merck), potassium permanganate (Merck), liquor ammonia (Merck), hydrogen peroxide, acetone, ethanol, doubled-distilled water, methylene blue dye.

Preparation of GO

Graphene oxide (GO) was prepared following the Modified Hummers method (William et al. 1958). Using this method, at first, 1 g natural flake graphite powder was taken in a 500 mL beaker and 23 mL concentrated H_2SO_4 was added to it. Then the mixture was subjected to magnetic stirrer for 48 h. After stirring, potassium permanganate was added slowly in ice-cold condition and the color has been changed from greenish to brown. Then, the whole dispersion was transferred into ice-cold water and after that hydrogen peroxide was added to make the complete reduction and the color turned from brown to pale yellow. Centrifugation was done to collect the precipitate, then washed several times with

Table 1 Summary of photocatalytic performance of $ZnCr_2O_4$ nanomaterials reported in recent papers till date

Photocatalyst	Synthetic procedure	Amt. of sample used	Dye used	Dye conc and amt	Irradiation light source	Irradiation time	% of degradation	Reference (year)
$ZnCr_2O_4$ NPs	Hydrothermal route	400 mg L^{-1}	Methylene blue	2.46 ppm and 400 mL	300-W medium-pressure Hg lamp	120 min	87	(Peng and Gao 2008)
ZnO–$ZnCr_2O_4$ nanolayered	Combustion technique	4000 mg L^{-1}	Acid orange 10	10.01 ppm and 200 mL	500-W tungsten lamp	180 min	99	(Thennarasu and Sivasamy 2015)
$ZnCr_2O_4$ dendrimer	Hydrothermal method	1000 mg L^{-1}	Eriochrome Black T	20 ppm and 50 mL	Ultraviolet radiation	120 min	91	(Sabet and Jahangiri 2018)
TiO_2–$ZnCr_2O_4$ core–shell NPs	Heterogeneous precipitation	1000 mg L^{-1}	Methylene blue	30 ppm and 50 mL	UV lamp (15 W, Philips)	120 min	99	(Salehi et al. 2018)
ZnS–$ZnCr_2O_4$ nanohybrid	Precipitation process	400 mg L^{-1}	Methyl orange	40 ppm, 100 mL	Tungsten-halogen lamp	105 min	96.88	(Palanisamy et al. 2020)
$ZnCr_2O_4$-rGO	Reflux and calcination	200 mg L^{-1}	Methylene blue	10 ppm and 50 mL	500-W tungsten lamp	70 min	96	Present work

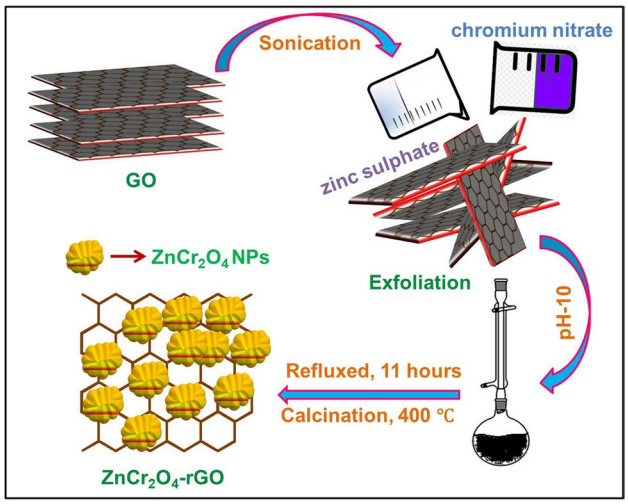

Scheme 1 Synthesis diagram of $ZnCr_2O_4$-rGO nanocomposites

10% HCl followed by distilled water. Finally, the precipitate was obtained as GO.

Synthesis of $ZnCr_2O_4$-rGO spinel nanoparticle

$ZnCr_2O_4$-rGO nanocomposites have been synthesized using graphene oxide (GO) sheet as growing substrate in the simple chemical process. At first, 0.364 g GO was dispersed in 120 mL distilled water and sonicated for 40 min for clear dispersion. Twenty milliliters of 0.35 (M) zinc sulfate and 20 mL 0.70 (M) chromium nitrate solution was added separately to this GO dispersion with the continuous stirring condition. The total solution is stirred for the next 20 min and then pH 10 was adjusted by adding liquor ammonia dropwise. Then the whole dispersion was subjected to reflux for 11 h after stirring for 3 h at 80 °C. The obtained product was filtered, washed with distilled water and ethanol, and finally dried at 80 °C under vacuum condition as shown in Scheme 1. Bare $ZnCr_2O_4$ nanoparticles was synthesized using polyvinylpyrrolidone (PVP) as a stabilizer instead of GO. The two dried samples were heated for 3 h at 500 °C for calcination.

Characterization techniques

The crystal structures of the composites were determined by the X-ray diffractometer BRUKER D8 ADVANCE and nature of the chemical bonding was investigated by Fourier transform infrared (FTIR) study using SHIMADZU IR Prestige-21. UV–Vis study and the photocatalytic activity studies were carried out by SHIMADZU UV-1800 spectrophotometer. The size and the morphological study of these nanocomposites were investigated by the scanning electron microscope (Model SIGMA-300). Photoluminescence (PL) study was done by Hitachi F-4500 spectrofluorometer.

Photocatalytic activity study

The photocatalytic performances of the two powdered samples $ZnCr_2O_4$ NPs and $ZnCr_2O_4$-rGO nanocomposites were investigated by the degradation of methylene blue (MB), an organic dye under a visible light irradiation. Ten milligrams of each sample was added to 50 mL MB dye solution (2.5 mg L^{-1}) separately and the mixture was stirred for 20 min to maintain adsorption–desorption equilibrium in dark environment. After 30 min of adsorption–desorption process, H_2O_2 was added to it and then exposed to visible light 500-W xenon lamp powers with constant stirring. UV–Vis absorption data were taken continuously after certain intervals of time, and it was found that the deep blue color of MB gradually disappears. Measuring the absorbance intensity during the photocatalytic degradation process, degree of degradation was calculated using this relation:

$$D\% = \frac{Ao - At}{Ao} X100 \quad (1)$$

Results and discussion

X-ray diffraction (XRD) patterns were collected to know the crystallographic structure of the synthesized samples $ZnCr_2O_4$ NPs and $ZnCr_2O_4$-rGO nanocomposite presented in the Fig. 1a. The characteristic peaks that appeared at 30.2°, 35.5°, 43.5°, 53.8°, 57.4°, 63.4°, and 75.2° correspond to the lattice planes of (220), (311), (400), (422), (511), (440), and (620) respectively. It is observed that all the XRD diffraction peaks for pure $ZnCr_2O_4$ sample recorded in the JCPDS 22–1107 are in a perfect match with the diffraction patterns of $ZnCr_2O_4$ in the composite material and also in $ZnCr_2O_4$ nanoparticles which confirm the formation of $ZnCr_2O_4$-rGO nanocomposite.

FTIR spectra of the synthesized sample $ZnCr_2O_4$-rGO nanocomposite and GO were recorded from 4000 to 400 cm^{-1}. In Fig. 1b, GO has the characteristic peaks at 3395, 1725, 1620, 1053 and 1230 cm^{-1} for the corresponding O–H, C = O, C = C, C–O stretching and C–O–C bending respectively (Sharma et al. 2017; Sudesh et al. 2013). But in the nanocomposite sample, the presence of two strong bands at 520 cm^{-1} and 623 cm^{-1} indicates the stretching vibrations of Cr–O and Zn–O bonds respectively. At the same time, the appearance of the peaks located at around 1121 (C–O stretching) and 1627 (C = C) cm^{-1} and lower intensity of the peak due to O–H stretching confirms the formation of the reduced graphene oxide along with the $ZnCr_2O_4$ nanoparticles.

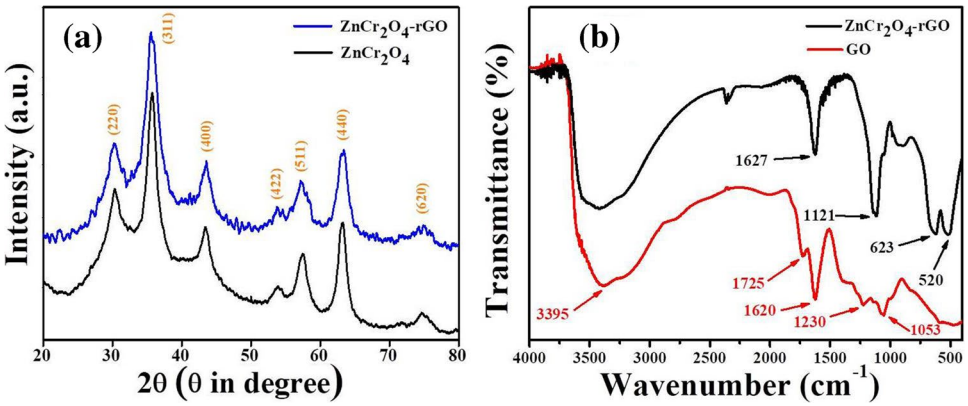

Fig. 1 **a** XRD patterns of $ZnCr_2O_4$ NPs and $ZnCr_2O_4$-rGO nanocomposite and **b** FTIR spectra of GO and $ZnCr_2O_4$-rGO nanocomposite

The absorption spectra of the $ZnCr_2O_4$-rGO nanocomposite was recorded from 200- 800 nm wavelength range as shown in Fig. 2. The peaks at around 270 nm and 355–390 nm can be assigned for the π-π* transition of aromatic C–C bond in graphene network and octahedral Cr^{3+} (d^3) ions respectively. The hump that arises near the visible region can be attributed to band gap absorption of $ZnCr_2O_4$ nanoparticles which is quite left shifted than the reported literature (Naz et al. 2016; Abdullah 2016). The absorption band gap can be estimated using the following Tauc relation (Zanatta 2019):

$$\alpha h\nu = A(h\nu - E_g)^n \tag{2}$$

where A is a constant and E_g is the absorption band gap of the material; n is a number which indicates the nature of electronic transition between valance band and conduction band, which have the values 1/2, 2, 3/2 and 3 corresponding to the allowed direct, allowed indirect, forbidden direct and forbidden indirect transitions respectively. It is well known that $ZnCr_2O_4$ responds to UV light but from the above equation, the plot of $(\alpha h\nu)^2$ vs. hν will give a divergence at an energy value E_g. The estimated band gap value from the plot for $ZnCr_2O_4$-rGO nanocomposite can be obtained by extrapolating the straight line to the energy axis at α = 0. The linear part shows that the mode of transition in this nanocomposite is direct in nature and the calculated band gap value was found to be 2.82 eV which is less than that of reported value of virgin $ZnCr_2O_4$ nanoparticles. This might be due to the strain that comes for the combination of graphene with nanoparticles after being formation of $ZnCr_2O_4$-rGO nanocomposite.

The morphology of virgin $ZnCr_2O_4$ and $ZnCr_2O_4$-rGO nanocomposite is analyzed by transmission electron microscopy. Virgin $ZnCr_2O_4$ forms by agglomeration of small particles around 15–20 nm as shown in Fig. 3a. The average particle size of $ZnCr_2O_4$ NPs in the composite (Fig. 3b) is smaller than that of virgin $ZnCr_2O_4$ NPs which is due to the presence of rGO surface. From the Fig. 3c, it is clearly shown that the $ZnCr_2O_4$ NPs are spread throughout the rGO sheet and the average particle size is approximately 4–7 nm (Fig. 3d) which is proven by particle size distribution curve as shown in Fig. 3e.

The EDX study of the synthesized samples has been carried out from the SEM images. Table 2 described the obtained results from Fig. 3f and Fig. S1 (supporting info) which showed the presence of the elements Zn, Cr, C and O in $ZnCr_2O_4$ NPs and $ZnCr_2O_4$-rGO nanocomposite respectively. Here, the weight percent of carbon is too much less

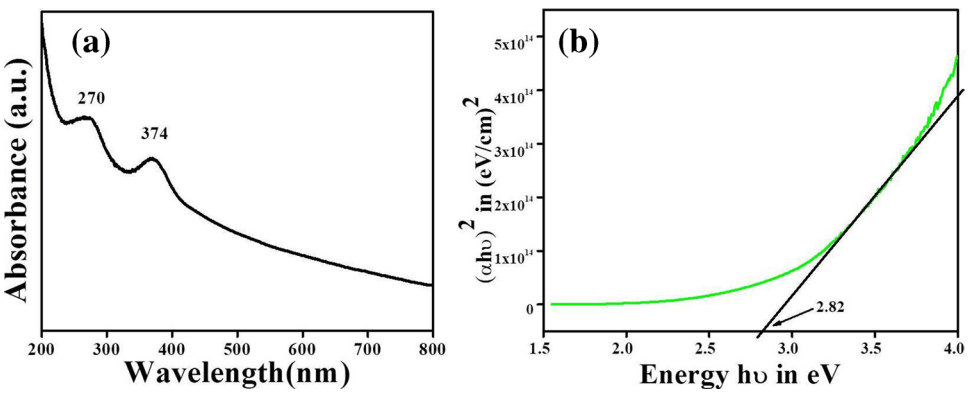

Fig. 2 **a** UV–Vis absorbance spectra $ZnCr_2O_4$-rGO nanocomposite, **b** Tauc's plot

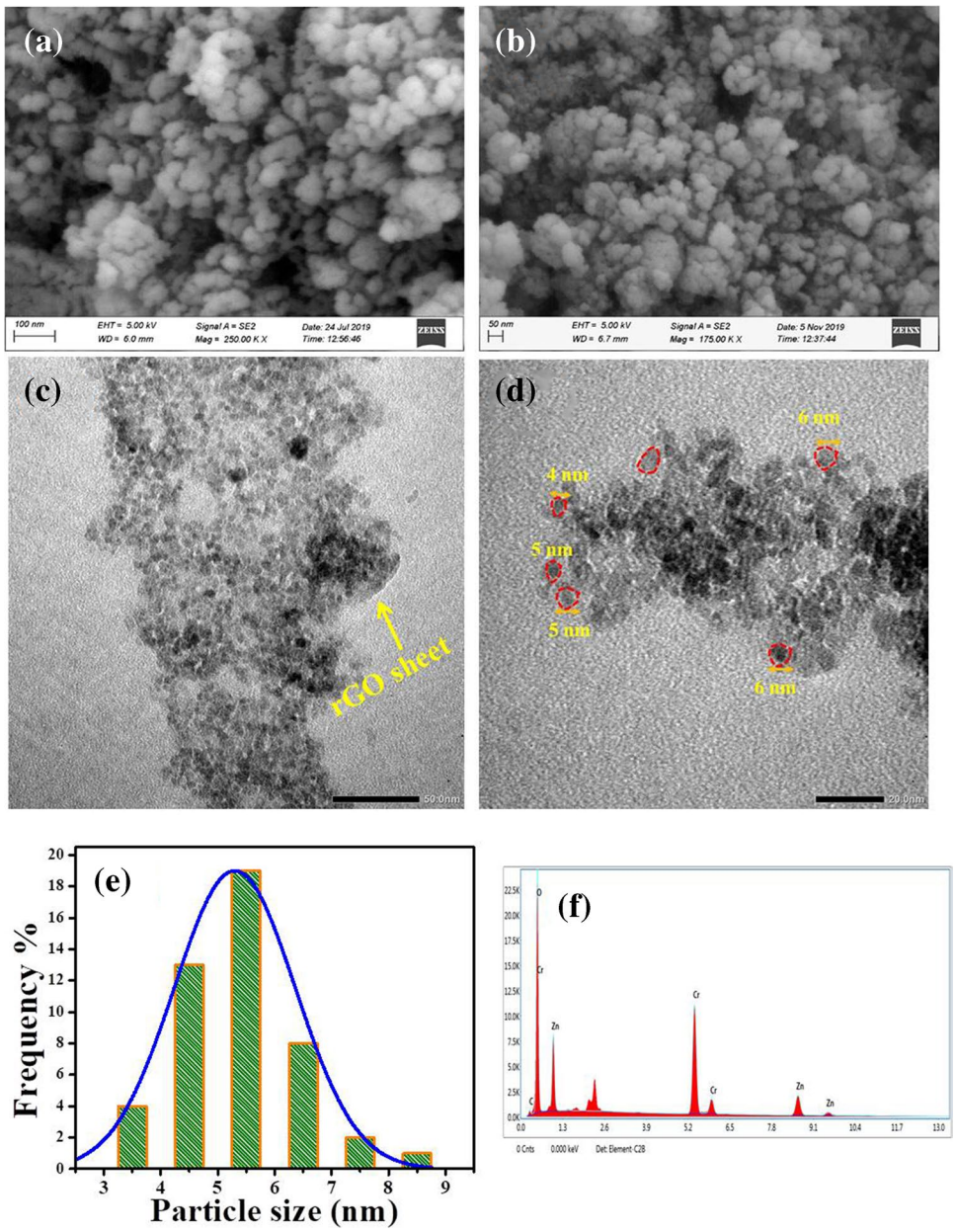

Fig. 3 FESEM images of **a** $ZnCr_2O_4$ NPs and **b** $ZnCr_2O_4$-rGO nanocomposite, **c**, **d** TEM images of $ZnCr_2O_4$-rGO nanocomposite, **e** particle distribution graph of $ZnCr_2O_4$-rGO nanocomposite, **f** EDX of $ZnCr_2O_4$-rGO nanocomposite

Table 2 EDX data of bare $ZnCr_2O_4$ NPs and $ZnCr_2O_4$-rGO nanocomposite

Sample	Element	Weight %	Atomic %
$ZnCr_2O_4$	Zn	21.18	9.23
	Cr	40.19	22.01
	O	38.63	68.76
$ZnCr_2O_4$-rGO	Zn	23.84	10.86
	Cr	42.47	24.32
	O	30.22	56.25
	C	3.46	8.57

because less amount of GO was used during the synthesis time.

The photoluminescence study of the nanomaterial is one of the important characterizations by which we can demonstrate the efficiency of migration and transfer of charge carriers and gives information about oxygen vacancies and defects as well as the separation and recombination of photo-induced charge carriers (Gao et al. 2019; Qian et al. 2018). Figure 4c shows the PL spectra for $ZnCr_2O_4$ and $ZnCr_2O_4$-rGO samples with an excitation wavelength of 249 nm. The main emission peak is centered at about 350–450 nm for the two samples. The PL emission intensity decreases slightly from $ZnCr_2O_4$ to $ZnCr_2O_4$-rGO nanocomposite. This suggests the enhanced photocatalytic

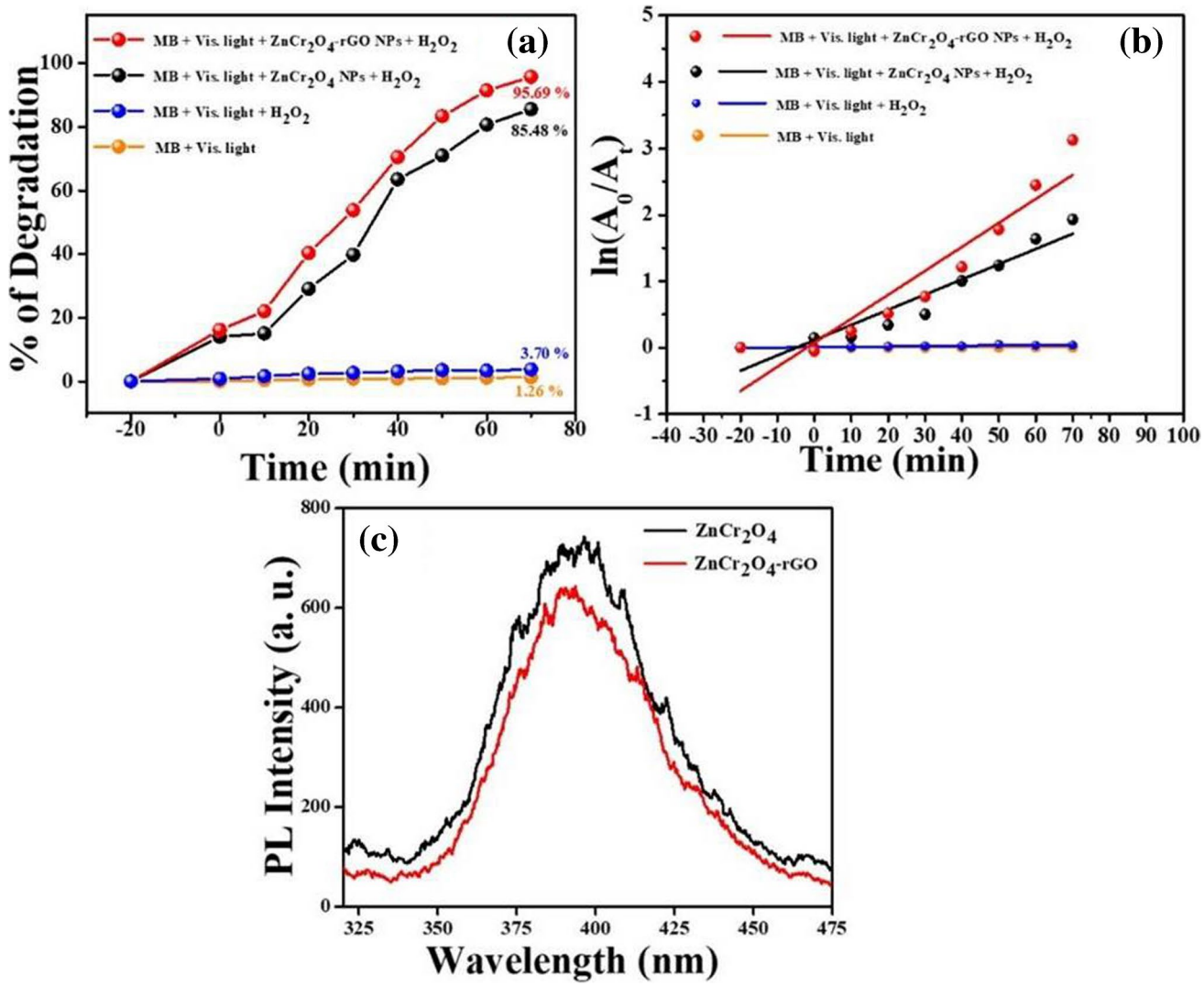

Fig. 4 **a** Photocatalytic degradation efficiency, **b** plot of ln (A_0/A_t) vs. time, **c** PL spectra of $ZnCr_2O_4$ NPs and $ZnCr_2O_4$-rGO nanocomposite

performance of $ZnCr_2O_4$-rGO compared to $ZnCr_2O_4$ because of lower recombination rate of photo-generated charge carriers in $ZnCr_2O_4$-rGO nanocomposite. Due to presence of rGO sheet in the nanocomposite material, the photo-generated electrons from the conduction band ($ZnCr_2O_4$) moves to the rGO surface and finally reduces the possibility of recombination of electron–hole pairs and photocatalytic activity increases as a result of lowering in the PL intensity.

Photocatalytic study

In order to evaluate the degradation efficiency of the two samples, the irradiation experiment was conducted by H_2O_2-assisted photolysis of MB. In Fig. 4a, it is shown that after visible light irradiation, the degradation of MB dye increases in the presence of H_2O_2 but this catalytic reaction enhances in greater extent when NPs are used as a catalyst. During the photocatalytic experiments, the nanocatalysts $ZnCr_2O_4$ and $ZnCr_2O_4$-rGO achieved 85.48% and 95.69% photodegradation after 70 min of visible light irradiation (Fig. 4a). This is due to the fact that the $ZnCr_2O_4$-rGO sample has a larger surface area than virgin $ZnCr_2O_4$ NPs because of the decreased size of $ZnCr_2O_4$ NPs after the addition of GO in nanocomposite. The concentration of MB gradually decreases and this reaction follows pseudo-first-order kinetics as shown in Eq. (3),

$$ln(A_0/A_t) = kt \tag{3}$$

where A_0 is the absorbance at $t = 0$ (initial MB absorbance), A_t is the absorbance at time $t = t$ (final MB absorbance), and k is the rate constant. A linear fit curve was obtained with ln (A_0/A_t) against illumination time and the

Table 3 Comparison of the degradation efficiency, the rate constant and relative correlation coefficient of different photo degradation experiments

Experiment	Sample	Degradation %	Rate (min^{-1})	R^2 value
MB + light	No	1.26	1.4×10^{-4}	0.9611
MB + light + H_2O_2	No	3.70	5.4×10^{-4}	0.7746
MB + light + H_2O_2 + $ZnCr_2O_4$	$ZnCr_2O_4$	85.48	2.28×10^{-2}	0.8956
MB + light + H_2O_2 + $ZnCr_2O_4$-rGO	$ZnCr_2O_4$-rGO	95.69	3.36×10^{-2}	0.8730

degradation rate constant was calculated for the samples $ZnCr_2O_4$ and $ZnCr_2O_4$-rGO as shown in Table 3.

Photocatalytic mechanism

In order to explain the H_2O_2-assisted photocatalytic activity, the possible photocatalytic route has been developed in Scheme 2. When the $ZnCr_2O_4$ NPs and $ZnCr_2O_4$-rGO nanocomposite photocatalysts were excited with photon energy, the electrons in the valence band (VB) transfer to the conduction band (CB) generating the same number of holes in VB as shown in Scheme 2. The photogenerated electrons can form superoxide radical anions ($O_2^{\cdot-}$) combining with dissolved O_2 and photogenerated holes transform the HO^- into $HO^{\cdot}$ radical. The recombination of holes (h^+) and electrons (e^-) has been considered an adverse process in photocatalysis. So, the probability of photocatalytic process has been improved by retardation of recombination process or increasing photocatalysis performance in the presence of other catalysts. Here H_2O_2 acts as an important role in this photocatalytic reaction (Baghriche et al. 2016) and it can behave as an electron acceptor and thus can form hydroxyl radicals through the following reaction.

First, the direct photolysis of H_2O_2 and generation of free radicals occur after the absorption of visible light (Wong et al. 2003) which is to be expected the dominant rate-enhancing mechanism in this process (Eq. 1). Another minor mechanism which has been preferred by Ollis et al. (1991) and Ilisz et al. (1998) may partially affect to the rate enhancement, in which H_2O_2 is recommended to be a better electron acceptor than oxygen. This would minimize the possibility of electron–hole recombination and can generate one hydroxyl radical as shown in Eq. **ii** (Gao et al. 2002), rather than the weaker $O_2^{\cdot-}$ radical (Eq. **v**). Finally, these generated radicals ($HO^{\cdot}$, $O_2^{\cdot-}$) are the main active species for the degradation of MB dye molecules. In this way of the dual catalysts, the nanocomposite and H_2O_2 can affect the degradation of MB dye.

Conclusions

Zinc chromite nanoparticles ($ZnCr_2O_4$ NPs) and graphene hybridized chromite nanocomposite ($ZnCr_2O_4$-rGO) were synthesized by the simple reflux condensation method. Different characterization techniques have confirmed the formation of the nanomaterial and the nanocomposite. Microscopic methods showed that the particle size of zinc chromite NPs in the nanocomposite is smaller than that of the bare one and this incident has raised due to combination

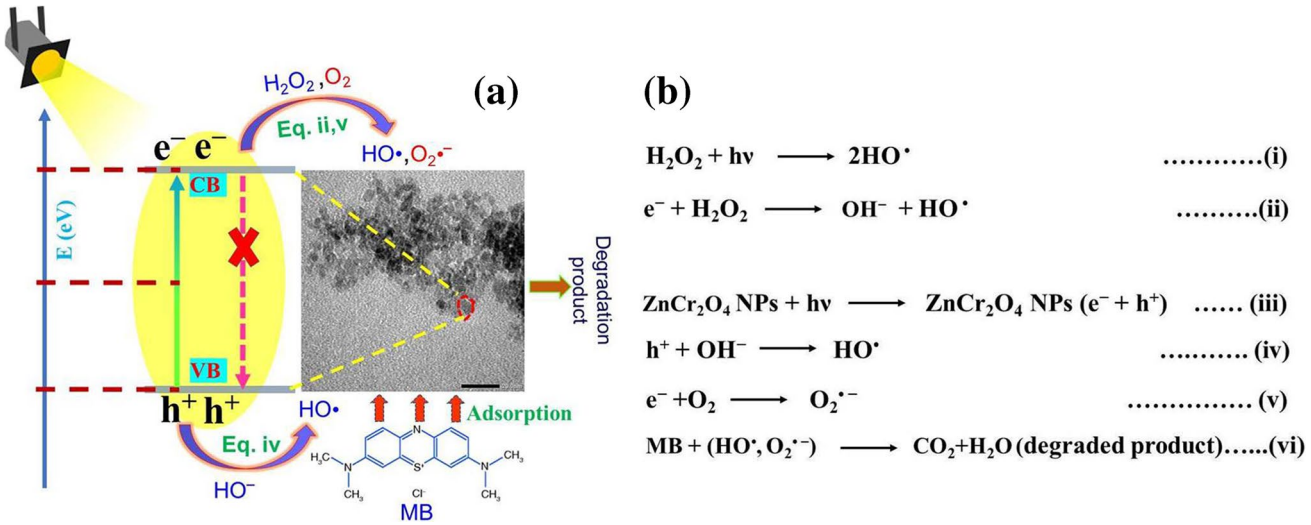

Scheme 2 **a**, **b** Pictorial and schematic representation of photocatalytic mechanism respectively

of rGO on the nanocomposite sample. The synthesized nanostructures exhibited excellent photocatalytic activity in presence of H_2O_2 and it is also supported by photoluminescence study and the band gap value. In a fixed time limit, $ZnCr_2O_4$-rGO nanocomposite showed approximately 96% degradation whereas the degradation efficiency is 85% in case of bare $ZnCr_2O_4$ NPs. It can be concluded that these nanophotocatalysts could be used extensively for the degradation of pollutants, photocatalytic disinfection and photocatalytic hydrogen generation processes.

Supplementary Information The online version contains supplementary material available at https://doi.org/10.1007/s11356-021-17105-1.

Acknowledgements K. T. acknowledges Swami Vivekananda Merit-Cum-Means Scholarship (Non-NET Junior Research Fellowship), Higher Education Department, Govt. of West Bengal for the financial support and P. D. acknowledges Bagati Shib Chandra Banerjee Girls' High School, Hooghly for permitting to continue her research work. We acknowledge University Science Instrumentation Center (USIC) for TEM and SEM facilities.

Author contribution Kartik Tantubay: writing—original draft; writing—review and editing; conceptualization; methodology; investigation.

Piu Das: validation, conceptualization, data curation, visualization, formal analysis, funding acquisition.

Moni Baskey Sen: Supervision, writing, and conceptualization.

Data availability The data that support the findings of this study are available from the authors.

Declarations

Ethical approval All procedures performed in studies involving human participants were in accordance with the ethical standards of the institutional and/or national research committee and with the 1964 Helsinki declaration and its later amendments or comparable ethical standards.

Consent to participate All participants voluntarily agreed to participate in this research study.

Consent to publish All participants voluntarily agreed to publish their research work in Springer journal.

Competing interests The authors declare no competing interests.

References

Abdullah OG (2016) Synthesis of single-phase zinc chromite nano-spinel embedded in polyvinyl alcohol films and its effects on energy band gap. J Mater Sci Mater Electron 27:12106–12111. https://doi.org/10.1007/s10854-016-5361-0

Amer AA, Reda SM, Mousa MA, Mohamed MM (2017) Mn_3O_4/graphene nanocomposites: outstanding performances as highly efficient photocatalysts and microwave absorbers. RSC Adv 7:826–839. https://doi.org/10.1039/c6ra24815b

An X, Yu JC (2011) Graphene-based photocatalytic composites. RSC Adv 1:1426–1434. https://doi.org/10.1039/C1RA00382H

Anshuman A, Yarahmadi SS, Vaidhyanathan B (2018) Enhanced catalytic performance of reduced graphene oxide–TiO_2 hybrids for efficient water treatment using microwave irradiation. RSC Adv 8:7709–7715. https://doi.org/10.1039/C8RA00031J

Baghriche O, Rtimi S, Pulgarin C, Kiwi J (2016) Polystyrene CuO/Cu_2O uniform films inducing MB-degradation under sunlight. Catal Today 284:77–83. https://doi.org/10.1016/j.cattod.2016.10.018

Chen Y, Chen L, Bai H, Li L (2013) Graphene oxide–chitosan composite hydrogels as broad-spectrum adsorbents for water purification. J Mater Chem A 1:1992–2001. https://doi.org/10.1039/C2TA00406B

Choudhary P, Yadav A, Varshney D (2017) Structural and optical studies of nanocrystalline $ZnCr_2O_4$ and $CoCr_2O_4$ Spinel. AIP Conf Proc 1832:0500511–0500513. https://doi.org/10.1063/1.4980284

Das P, Ghosh S, Ghosh R, Dam S, Sen MB (2018) *Madhuca longifolia* plant mediated green synthesis of cupric oxide nanoparticles: a promising environmentally sustainable material for waste water treatment and efficient antibacterial agent. J Photochem Photobiol B Biol 189:66–73. https://doi.org/10.1016/j.jphotobiol.2018.09.023

Das P, Ghosh S, Sen MB (2019) Heterogeneous catalytic reduction of 4-nitroaniline by RGO-Ni nanocomposite for water resource management. J Mater Sci Mater 30:1–7. https://doi.org/10.1007/s10854-019-02323-8

Das P, Tantubay K, Ghosh R, Dam S, Sen MB (2021) Transformation of CuS/ZnS nanomaterials to an efficient visible light photocatalyst by 'photosensitizer' graphene and the potential antimicrobial activities of the nanocomposites. Environ Sci Pollut Res 1-14. https://doi.org/10.1007/s11356-021-14068-1

Dong S, Feng J, Fan M, Pi Y, Hu L, Han X, Liu M, Sun J, Sun J (2015) Recent developments in heterogeneous photocatalytic water treatment using visible-light-responsive photocatalysts: a review. RSC Adv 5:14610–14630. https://doi.org/10.1039/C4RA13734E

Dubey SP, Nguyen TTM, Kwon YN, Lee C (2015) Synthesis and characterization of metal-doped reduced graphene oxide composites and their application in removal of *Escherichia coli*, arsenic and 4-nitrophenol. J Ind Eng Chem 29:282–288. https://doi.org/10.1016/j.jiec.2015.04.008

Dumitru R, Manea F, Păcurariu C, Lupa L, Pop A, Cioablă A, Surdu A, Ianculescu A (2018) Synthesis, characterization of nanosized $ZnCr_2O_4$ and its photocatalytic performance in the degradation of humic acid from drinking water. Catalysts 8:210–225. https://doi.org/10.3390/catal8050210

Gao M, Wu X, Qiu H, Zhang Q, Huang K, Feng S, Yang Y, Wang T, Zhao B, Liu Z (2018) Reduced graphene oxide-mediated synthesis of Mn_3O_4 nanomaterials for an asymmetric supercapacitor cell. RSC Adv 8:20661–20668. https://doi.org/10.1039/c8ra00092a

Gao R, Stark J, Bahnemann D, Rabani J (2002) Quantum yields of hydroxyl radicals in illuminated TiO_2 nanocrystallite layers. J Photochem Photobiol A Chem 148:387–391. https://doi.org/10.1016/S1010-6030(02)00066-7

Gao W, Lu J, Zhang S, Zhang X, Wang Z, Qin W, Wang J, Zhou W, Liu H, Sang Y (2019) Suppressing photoinduced charge recombination via the lorentz force in a photocatalytic system. Adv Sci 6:1901244–1901250. https://doi.org/10.1002/advs.201901244

Ghosh D, Dutta U, Haque A, Mordvinova NE, Lebedev OI, Pal K, Gayen A, Seikh MM, Mahata P (2018) Ultra high sensitivity of luminescent $ZnCr_2O_4$ nanoparticles toward aromatic nitro explosives sensing. Dalton Trans 47:5011–5018. https://doi.org/10.1039/C8DT00047F

Ghosh S, Das P, Bairy B, Ghosh R, Dam S, Sen MB (2021a) Exploration of photoreduction ability of reduced graphene oxide–cadmium sulphide hetero-nanostructures and their intensified activities against harmful microbes. J Mater Sci 56:16928–16944. https://doi.org/10.1007/s10853-021-06422-y

Ghosh S, Das P, Sen MB (2021b) Plant extract assisted synthesis of reduced graphene oxide sheet and the photocatalytic performances on cationic and anionic dyes to decontaminate wastewater. Adv Nat Sci Nanosci Nanotechnol 12:015008–015016. https://doi.org/10.1088/2043-6254/abde41

Gnanamoorthy G, Ramar K, Ali D, Yadavd VK, Sureshbabu K, Narayanan V (2020) A series of $ZnCo_2O_4$/rGO/Pt nanocubes with excellent photocatalytic activity towards visible light. Chem Phys Lett 759:137988–137996. https://doi.org/10.1016/j.cplett.2020.137988

Gupta S, Joshi P, Narayan J (2020) Electron mobility modulation in graphene oxide by controlling carbon melt lifetime. Carbon 170:327–337. https://doi.org/10.1016/j.carbon.2020.07.073

Gusain R, Kumar P, Sharma OP, Jain SL, Khatr OP (2016) Reduced graphene oxide-CuO nanocomposites for photocatalytic conversion of CO_2 into methanol under visible light irradiation. Appl Catal B Environ 181:352–362. https://doi.org/10.1016/j.apcatb.2015.08.012

Ilisz I, Föglein K, Dombi A (1998) The photochemical behavior of hydrogen peroxide in near UV-irradiated aqueous TiO_2 suspensions. J Mol Catal 135:55–61. https://doi.org/10.1016/S1381-1169(97)00296-3

Jaleh B, Karami S, Sajjadi M, Feizi MB, Azizian S, Nasrollahzadeh M, Varma RS (2019) Laser-assisted preparation of Pd nanoparticles on carbon cloth for the degradation of environmental pollutants in aqueous medium. Chemosphere 246:125755–125773. https://doi.org/10.1016/j.chemosphere.2019.125755

Kalisamy P, Lallimathi M, Suryamathi M, Palanivel B, Venkatachalam M (2020) ZnO-embedded S-doped g-C_3N_4 heterojunction: mediator-free Z-scheme mechanism for enhanced charge separation and photocatalytic degradation. RSC Adv 10:28365–28375. https://doi.org/10.1039/D0RA04642F

Kocijan M, Ćurković L, Ljubas D, Mužina K, Bačić I, Radoševic T, Podlogar M, Bdikin I, Irurueta GO, Hortigüela MJ, Gonçalves G (2021) Graphene-based TiO_2 nanocomposite for photocatalytic degradation of dyes in aqueous solution under solar-like radiation. Appl Sci 11:3966-3980. https://doi.org/10.3390/app11093966

Krishnan S, Murugesan S, Vasanthakumar V, Priyadharsan A, Alsawalha M, Alomayri T, Yuan B (2020) Facile green synthesis of $ZnFe_2O_4$/rGO nanohybrids and evaluation of its photocatalytic degradation of organic pollutant, photo antibacterial and cytotoxicity activities. Colloids Surf A Physicochem Eng Asp 611:125835–125870. https://doi.org/10.1016/j.colsurfa.2020.125835

Kumar KV, Chakra CHS (2017) Synthesis and structural characterization of $ZnCr_2O_4$ nanoparticles prepared by citrate-gel auto combustion method. Asian J Phys Chem Sci 2:1–7. https://doi.org/10.9734/AJOPACS/2017/34683

Kumar S, Kaushik RD, Upadhyay GK, Purohit LP (2021) rGO-ZnO nanocomposites as efficient photocatalyst for degradation of 4-BP and DEP using high temperature refluxing method in in-situ condition. J Hazard Mater 406:124300. https://doi.org/10.1016/j.jhazmat.2020.124300

Mohazzab BF, Jaleh B, Nasrollahzadeh M, Khazalpour S, Sajjadi M, Varma RS (2020) Upgraded valorization of biowaste: Laser-assisted synthesis of Pd/Calcium lignosulfonate nanocomposite for hydrogen storage and environmental remediation. ACS Omega 5:5888–5899. https://doi.org/10.1021/acsomega.9b04149

Nafiey AL, Kumar A, Kumar M, Addad A, Sieber B, Szunerits S, Boukherroub R, Jain SL (2017) Nickel oxide nanoparticles grafted on reduced graphene oxide (rGO/NiO) as efficient photocatalyst for reduction of nitro aromatics under visible light irradiation. J Photochem Photobiol A Chem 336:198–207. https://doi.org/10.1016/j.jphotochem.2016.12.023

Naghdi S, Sajjadi M, Nasrollahzadeh M, Rhee KY, Sajadi SM, Jaleh B (2018) Cuscuta reflexa leaf extract mediated green synthesis of the Cu nanoparticles on graphene oxide/manganese dioxide nanocomposite and its catalytic activity toward reduction of nitroarenes and organic dyes. J Taiwan Inst Chem Eng 000:1–16. https://doi.org/10.1016/j.jtice.2017.12.017

Nasrollahzadeh M, Jaleh B, Baran T, Varma RS (2019) Efficient degradation of environmental contaminants using Pd-RGO nanocomposite as a retrievable catalyst. Clean Technol Environ Policy 22:325–335. https://doi.org/10.1007/s10098-019-01784-z

Nasrollahzadeh M, Sajjadi M, Iravani S, Varm RS (2020) Carbon-based sustainable nanomaterials for water treatment: state-of-art and future perspectives. Chemosphere 263:128005–128020. https://doi.org/10.1016/j.chemosphere.2020.12

Nasrollahzadeh M, Sajjadi M, Iravani S, Varma RS (2021a) Green-synthesized nanocatalysts and nanomaterials for water treatment: current challenges and future perspectives. J Hazard Mater 401:1–97. https://doi.org/10.1016/j.jhazmat.2020.123401

Nasrollahzadeh M, Sajjadi M, Iravani S, Varma RS (2021b) Starch, cellulose, pectin, gum, alginate, chitin and chitosan derived (nano) materials for sustainable water treatment: a review. Carbohydr Polym 251:116986–1191017. https://doi.org/10.1016/j.carbpol.2020.116986

Naz S, Durrani SK, Mehmood M, Nadeem M (2016) Hydrothermal synthesis, structural and impedance studies of nanocrystalline zinc chromite spinel oxide material. J Saudi Chem Soc 20:585–593. https://doi.org/10.1016/j.jscs.2014.12.007

Nguyen MA, Zahran EM, Wilbon AS, Besmer AV, Cendan VJ, Ranson WA, Lawrence RL, Cohn JL, Bachas LG, Knecht MR (2016) Converting light energy to chemical energy: A new catalytic approach for sustainable environmental remediation. ACS Omega 1:41–51. https://doi.org/10.1021/acsomega.6b00076

Ollis DF, Pelizzetti E, Serpone N (1991) Photocatalyzed destruction of water contaminants. Environ Sci Technol 25:1522–1529. https://doi.org/10.1021/es00021a001

Omidvar A, Jaleh B, Nasrollahzadeh M (2017a) Preparation of the GO/Pd nanocomposite and its application for the degradation of organic dyes in water. J Colloid Interface Sci 496:44–50. https://doi.org/10.1016/j.jcis.2017.01.113

Omidvar A, Jaleh B, Nasrollahzadeh M, Dasmeh HR (2017b) Fabrication, characterization and application of GO/Fe_3O_4/Pd nanocomposite as a magnetically separable and reusable catalyst for the reduction of organic dyes. Chem Eng Res Des 121:339–347. https://doi.org/10.1016/j.cherd.2017.03.026

Padhi DK, Panigrahi TK, Parida K, Singh SK, Mishra PM (2017) Green synthesis of Fe_3O_4/RGO nanocomposite with enhanced photocatalytic performance for Cr (VI) reduction, phenol degradation, and antibacterial activity. ACS Sustain Chem Eng 5:10551–10562. https://doi.org/10.1021/acssuschemeng.7b02548

Palanisamy G, Pazhanivel T, Bhuvaneswari K, Bharathi G, Marimuthu G, Maiyalagan T (2020) Spinel oxide $ZnCr_2O_4$ incorporated with ZnS quantum dots for application on visible light driven photocatalyst Azo dye degradation. Colloids Surf A Physicochem Eng Asp 590:124505–124536. https://doi.org/10.1016/j.colsurfa.2020.124505

Peng C, Gao L (2008) Optical and photocatalytic properties of spinel $ZnCr_2O_4$ nanoparticles synthesized by a hydrothermal route. J Am Ceram Soc 91:2388–2390. https://doi.org/10.1111/j.1551-2916.2008.02417.x

Pokhrel S, Jeyaraj B, Nagaraja KS (2003) Humidity-sensing properties of $ZnCr_2O_4$–ZnO composites Mater Lett 57:3543–3548. https://doi.org/10.1016/S0167-577X(03)00122-8

Qian R, Zong H, Schneider J, Zhou G, Zhao T, Li Y, Yang J, Bahnemann DW, Pan JH (2018) Charge carrier trapping, recombination and transfer during TiO_2 photocatalysis: An overview. Catal Today 335:78–90. https://doi.org/10.1016/j.cattod.2018.10.053

Rahaman AB, Sarkar A, Singha T, Chakraborty K, Dutta S, Pal T, Ghosh S, Datta PK, Banerjee D (2020) Electrical transport properties and ultrafast optical nonlinearity of rGO–metal chalcogenide

ensembles. Nanoscale Adv 2:1573–1582. https://doi.org/10.1039/c9na00728h

Sabet M, Jahangiri H (2018) The effects of surfactant on the structure of $ZnCr_2O_4$ dendrimer like nanostructures used in degradation of Eriochrome Black T. Mater Res Express 5:015035. https://doi.org/10.1088/2053-1591/aaa442

Salehi M, Eshaghi A, Tajizadegan H (2018) Synthesis and characterization of $TiO_2/ZnCr_2O_4$ core-shell structure and its photocatalytic and antibacterial activity. J Alloys Compd 778(148–155):v. https://doi.org/10.1016/j.jallcom.2018.11.025

Sen MB, Ghosh S (2017) Enhanced sunlight photocatalytic activity of silver nanoparticles decoratedon reduced graphene oxide sheet. Korean J Chem Eng 34:2079–2085. https://doi.org/10.1007/s11814-017-0090-5

Shang J, Hao W, Lv X, Wang T, Wang X, Du Y, Dou S, Xie T, Wang D, Wang J (2014) Bismuth oxybromide with reasonable photocatalytic reduction activity under visible light. ACS Catal 4:954–961. https://doi.org/10.1021/cs401025u

Sharma N, Sharma V, Jain Y, Kumari M, Gupta R, Sharma SK, Sachdev K (2017) Synthesis and characterization of graphene oxide (GO) and reduced graphene oxide (rGO) for gas sensing application. Macromol Symp 376:1700006–1700010. https://doi.org/10.1002/masy.201700006

Singh PK, Kuo KY, Lee JT, Hsiao PH, Juan JC, Duong HP, Chen CY (2021) Synergistic absorbents based on $SnFe_2O_4$@ZnO nanoparticles decorated with reduced graphene oxide for highly efficient dye adsorption at room temperature. RSC Adv 11:17840–17848. https://doi.org/10.1039/d1ra02317a

Sudesh KN, Das S, Bernhard C, Varma GD (2013) Effect of graphene oxide doping on superconducting properties of bulk MgB_2. Supercond Sci Technol 26:095008–095015. https://doi.org/10.1088/0953-2048/26/9/095008

Tajizadegan H, Heidary A, Torabi O, Golabgir MH, Jamshidi A (2016) Synthesis and characterization of $ZnCr_2O_4$ nanospinel prepared via homogeneous precipitation using urea hydrolysis. Int J Appl Ceram Technol 13:289–294. https://doi.org/10.1111/ijac.12440

Tantubay K, Das P, Sen MB (2020) Ternary reduced graphene oxide–CuO/ZnO nanocomposite as a recyclable catalyst with enhanced reducing capability. J Environ Chem Eng 8:103818–103824. https://doi.org/10.1016/j.jece.2020.103818

Thennarasu G, Sivasamy A (2015) Synthesis and characterization of nanolayered $ZnO/ZnCr_2O_4$ metal oxide composites and its photocatalytic activity under visible light irradiation. J Chem Technol Biotechnol 90:514–524. https://doi.org/10.1002/jctb.4343

Wang Y, An T, Yan N, Yan Z, Zhao B, Zhao F (2020) Nanochromates MCr_2O_4(M = Co,Ni, Cu, Zn): preparation, characterization, and catalytic activity on the thermal decomposition of fine AP and CL-20. ACS Omega 5:327–333. https://doi.org/10.1021/acsomega.9b02742

William S, Hummers J, Offeman RE (1958) Preparation of graphitic oxide. J Am Chem Soc 80:1339. https://doi.org/10.1021/ja01539a017

Wong CC, Chu W (2003) The hydrogen peroxide-assisted photocatalytic degradation of alachlor in TiO_2 suspensions. Environ Sci Technol 37:2310–2316. https://doi.org/10.1021/es020898n

Yu L, Wang L, Sun X, Ye D (2017) Enhanced photocatalytic activity of rGO/TiO_2 for the decomposition of formaldehyde under visible light irradiation. J Environ Sci 73:138–146. https://doi.org/10.1016/j.jes.2018.01.022

Zanatta AR (2019) Revisiting the optical bandgap of semiconductors and the proposal of a unified methodology to its determination. Sci Rep 9(11225):1–12. https://doi.org/10.1038/s41598-019-47670-y